Prevalence of Novel *MAGED2* Mutations in Antenatal Bartter Syndrome

Anne Legrand, Cyrielle Treard, Isabelle Roncelin, Sophie Dreux, Aurélia Bertholet-Thomas, Françoise Broux, Daniele Bruno, Stéphane Decramer, Georges Deschenes, Djamal Djeddi, Vincent Guigonis, Nadine Jay, Tackwa Khalifeh, Brigitte Llanas, Denis Morin, Gilles Morin, François Nobili, Christine Pietrement, Amélie Ryckewaert, Rémi Salomon, Isabelle Vrillon, Anne Blanchard, and Rosa Vargas-Poussou

Abstract

Background and objectives Mutations in the *MAGED2* gene, located on the X chromosome, have been recently detected in males with a transient form of antenatal Bartter syndrome or with idiopathic polyhydramnios. The aim of this study is to analyze the proportion of the population with mutations in this gene in a French cohort of patients with antenatal Bartter syndrome.

Design, setting, participants, & measurements The French cohort of patients with antenatal Bartter syndrome encompasses 171 families. Mutations in genes responsible for types 1–4 have been detected in 75% of cases. In patients without identified genetic cause (n=42), transient antenatal Bartter syndrome was reported in 12 cases. We analyzed the *MAGED2* gene in the entire cohort of negative cases by Sanger sequencing and retrospectively collected clinical data regarding pregnancy as well as the postnatal outcome for positive cases.

Results We detected mutations in *MAGED2* in 17 patients, including the 12 with transient antenatal Bartter syndrome, from 16 families. Fifteen different mutations were detected (one whole deletion, three frameshift, three splicing, three nonsense, two inframe deletions, and three missense); 13 of these mutations had not been previously described. Interestingly, two patients are females; in one of these patients our data are consistent with selective inactivation of chromosome X explaining the severity. The phenotypic presentation in our patients was variable and less severe than that of the originally described cases.

Conclusions *MAGED2* mutations explained 9% of cases of antenatal Bartter syndrome in a French cohort, and accounted for 38% of patients without other characterized mutations and for 44% of male probands of negative cases. Our study confirmed previously published data and showed that females can be affected. As a result, this gene must be included in the screening of the most severe clinical form of Bartter syndrome.

Clin J Am Soc Nephrol 13: 242–250, 2018. doi: https://doi.org/10.2215/CJN.05670517

Due to the number of contributing authors, the affiliations are provided in the Supplemental Material.

Correspondence: Dr. Rosa Vargas-Poussou, Département de Génétique, Hôpital Européen George Pompidou, 20–40 Rue Leblanc, 75015 Paris, France. Email: rosa.vargas@aphp.fr

Introduction

Bartter syndromes are autosomal recessive salt-losing tubulopathies caused by defective salt reabsorption. They are characterized by hypokalemia, metabolic alkalosis, and secondary hyperaldosteronism with normal or low BP (1,2). Bartter syndromes are classified by phenotype (antenatal, classic) or genotype (types 1–4). Antenatal Bartter syndrome is the most severe form, characterized by polyhydramnios, premature birth, life-threatening episodes of neonatal salt and water loss, hypercalciuria, and early-onset nephrocalcinosis (3). Classic Bartter syndrome occurs in infancy or early childhood and is characterized by salt wasting and hypokalemia, leading to polyuria, polydipsia, volume contraction, muscle weakness, growth retardation, and sometimes nephrocalcinosis (4). Bartter syndrome types 1, 2, and 3 are caused by mutations of genes expressed in the thick ascending limb of the loop of Henle encoding the luminal Na^+-K^+-$2Cl^-$ cotransporter or NKCC2 (*SLC12A1*; OMIM #601678), the luminal K^+ channel ROMK (*KCNJ1*; OMIM #241200), and the basolateral chloride channel ClC-Kb (*CLCNKB*; OMIM #607364) (5–8). Loss-of-function mutations of *BSND*, encoding barttin, an essential β subunit for chloride channels, cause Bartter syndrome type 4a with sensorineural deafness (OMIM #602522) (8). Simultaneous mutations of *CLCNKB* and *CLCNKA* cause type 4b Bartter syndrome (OMIM #613090) (9). In recent work, Laghmani *et al.* (10) analyzed by exome sequencing one family with three male patients having transient antenatal Bartter syndrome and identified a variant in the *MAGED2* gene, which cosegregated with the disease. Subsequent sequencing of other male patients with transient antenatal Bartter syndrome or with recurrent idiopathic polyhydramnios confirmed the presence of *MAGED2* mutations (10). *MAGED2* is located on the X chromosome and encodes melanoma-associated antigen D2 (MAGE-D2), which is expressed in the thick ascending limb of the loop of Henle and the distal

convoluted tubules in the developing and adult kidney. The authors showed lower expression of NKCC2 and NCC cotransporters in fetal tubular cells affected by *MAGED2* mutations; NCC is the sodium-chloride cotransporter of the distal convoluted tubule and loss-of-function mutations in the corresponding gene, *SLC12A3*, are responsible for Gitelman syndrome (11). The lower expression of NKCC2 and NCC has been explained by the interaction of MAGE-D2 protein with the chaperone protein, Hsp40, or with the G protein subunit, Gs-α, which may reduce the generation of cAMP. The decreased function of NKCC2 and NCC will be responsible for salt-losing tubulopathy with polyuria and polyhydramnios.

The aim of this study is to analyze the proportion of *MAGED2* mutations in the 42 genetically unresolved cases of our French cohort of antenatal Bartter syndrome. We also compare the phenotype with the four other types of antenatal Bartter syndromes to determine if it could be clinically distinguished in the perinatal period.

Materials and Methods

Patients

Patients with antenatal Bartter syndrome were referred from different pediatric nephrology services in France to the Genetics Department of the Georges Pompidou European Hospital (Paris, France) from January of 2000 to April of 2016 in order to genetically confirm the clinical diagnosis. Patients that were genetically negative for *SLC12A1*, *KCNJ1*, *CLCNKB*, and *BSND* were included in this study. The cohort includes 171 patients, with ethnic composition: white (56%), North African (21%), Middle East (12%), African (9%), and others (2%). Antenatal Bartter syndrome was diagnosed on the basis of the presence of polyhydramnios during pregnancy and losing salt tubulopathy in the neonatal period. Among antenatal Bartter syndrome, the transient form was defined as a regression of clinical symptoms and normalization of biologic parameters allowing the arrest of treatment. Data were retrospectively collected and included clinical and biologic findings during pregnancy, at diagnosis in the neonatal period, and throughout the follow-up. Informed consents for genetic study were obtained and genetic testing was performed in accordance with French legislation on genetic diagnostics tests (French bioethics law no. 2004–800).

Genetic Analysis

The Qiamp DNA Blood Midi kit (Qiagen, Hilden, Germany) was used according to the manufacturer's instructions to extract genomic DNA from leukocyte pellets.

Detection of Point Mutations

MAGED2 coding exons and the flanking intronic sequences were amplified by PCR with specific primers (conditions on request) and then sequenced using BigDye Terminator kit v3.1 cycle sequencing kits and run on an ABI Prism 3730XL DNA Analyzer (Life Technologies, Foster City, CA). DNA variants were identified using Sequencher software (Gene Codes Corporation, Ann Arbor, MI).

Unreported missense variants were interpreted with *in silico* prediction tools (SIFT: http://www.Blocks.fhcrc.org/sift/SIFT.html, PolyPhen-2: http://genetics.bwh.harvard.edu/pph/, and MutationTaster: http://www.mutationtaster.org/documentation.html), and previously unreported splicing variants were interpreted with MaxEntScan and SpliceSiteFinder. The frequencies in the general population of all variants were determined using the ExAC database (http://exac.broadinstitute.org/gene/ENSG00000091262).

Detection of Large Rearrangements

A *MAGED2* multiplex ligation–dependent probe amplification (MLPA) assay was developed to detect large rearrangement in one case with suspected deletion on the basis of nonamplification by PCR. The probes were designed according to the manufacturer's criteria: Eight probes were designed to hybridize to the coding exons with the exception of exons 4 and 9 for which no specific probes could be found (conditions on request). Our own probes were combined with the SALSA MLPA P300 Human reference probemix and EK-FAM MLPA reagent kit (MRC-Holland, Amsterdam, The Netherlands), according to the manufacturer's recommendations (http://www.mlpa.com). Fragments were detected using an ABI 3730XL DNA Analyzer with ROX500 (Life Technologies) as an internal size standard. Genemapper (Life Technologies) and Coffalyzer (MRC-Holland) softwares were used to analyze the MLPA fragments.

Detection of X-Inactivation

The X-inactivation patterns of female carriers were investigated by studying the polymorphic trinucleotide CAG repeat in the first exon of *HUMARA*, the gene encoding the human androgen receptor. First, 500 ng of DNA was digested using methylation-sensitive restriction enzymes (*Hpa*II and *Hha*I) whose cleavage sites are close to the CAG repeat element in the first exon of the *HUMARA* gene. Both digested and undigested DNA samples were amplified by the PCR method using primers that included the *Hpa*II and *Hha*I cleavage sites and the CAG repeat element, as reported in Allen *et al.* (12). The forward primer was modified with fluorescein (6′-FAM). In digested samples, amplification occurred only if the restriction sites were methylated. The PCR products were resolved by electrophoresis with ROX400 (Life Technologies) in an ABI 3730XL DNA Analyzer, and peak heights were analyzed using Genemapper. Triplicate samples were assayed for each female carrier to increase data accuracy. In addition, one control male sample was included to control for complete digestion. The peak height values of the digested samples were corrected for amplification efficiency by using the peak height values of the undigested samples. The ratios of the skewed X-inactivation in digested samples were then calculated by normalizing the sum of the two alleles to 100%. The X-inactivation pattern was classified as random (allele ratios 50:50%–65:35%), moderately skewed (ratios 65:35%–80:20%), highly skewed (ratios 80:20%–90:10%), or extremely skewed (ratios 90:10%–100:0%).

Statistical Analyses

Data were analyzed with GraphPad Prism Software (La Jolla, CA). For transient Bartter, descriptive statistics were used. To compare transient Bartter with the other four groups of antenatal Bartter, Kruskal–Wallis tests were used. In cases of statistical significance, Mann–Whitney *U* tests were used for pairwise comparisons.

Results

Genetic Studies

In the French cohort of antenatal Bartter syndrome (n=171 families), 75% of the cases corresponded to types 1–4. Analysis of the *MAGED2* gene in the remaining (n=42) negative cases allowed us to detect fifteen different mutations in 17 patients from 16 families. Within the 17 cases, 12 had clinical transient antenatal Bartter syndrome; three corresponded to one medical termination of pregnancy and two early deaths and two were confirmed to be transient, retrospectively. Thus, *MAGED2* mutations were present in 9% of cases of antenatal Bartter syndrome in our cohort (Figure 1).

The 15 mutations detected included three missense, two inframe deletions, three nonsense, three splicing, three frameshift, and one whole deletion. Thirteen of these mutations had not been previously described (Supplemental Figure 1, Table 1) and were absent from the ExAC database. Absence of PCR amplification in the F16 proband suggested a gene deletion, which was confirmed by MLPA (Supplemental Figure 2). Two of the novel missense variations, p.Arg446His and p.Val456Phe, affected conserved amino acids and were predicted to be pathogenic by the three tools used for *in silico* analysis (Supplemental Table 1). The novel inframe deletion was in the same region as the previously described one. The three splice-site mutations, two of which (introns 7 and 11) result in frameshift, disrupted the obligatory consensus donor or acceptor splice site and were likely to cause exon skipping (Table 1).

Analyses of 12 mothers showed that ten were heterozygous carriers and in two cases the mutation was *de novo*. Samples of five additional females were also analyzed: sisters of probands F2 and F10, for whom pregnancies coursed with polyhydramnios, and one sister of proband F7 and two sisters of proband F9 with normal pregnancies. Four of these females were heterozygous for the familial mutations; the exception was a sister of proband F9.

The X-inactivation pattern ratio was studied on the basis of methylation-specific PCR (Table 2). Families including more than one female patient (n=5) were analyzed in order to compare the X-inactivation pattern and the phenotype in the same family. Only data generated with *Hha*I were shown because reproducibility was better than with *Hpa*II. In families F2 and F12, two females were affected. In family F10, one female was diagnosed with polyhydramnios at delivery at 40 weeks of gestation; she did not present with transient antenatal Bartter syndrome. Unfortunately, her X-inactivation pattern ratio was uninterpretable. In F2, the values of relative X-inactivation were 94% for the normal allele and 6% for the mutated allele, whereas the mutated allele was mainly inactive in the asymptomatic mother (Supplemental Figure 3A). The X-inactivation pattern was extremely skewed and this bias likely explains the severity of the phenotype in this female patient. In F12, the mother was uninformative because she was homozygous for the studied polymorphism. Surprisingly, the X-inactivation pattern was random in the daughter.

In families F7 and F9, asymptomatic daughters harbored heterozygous *MAGED2* mutations: in F7, the X-inactivation

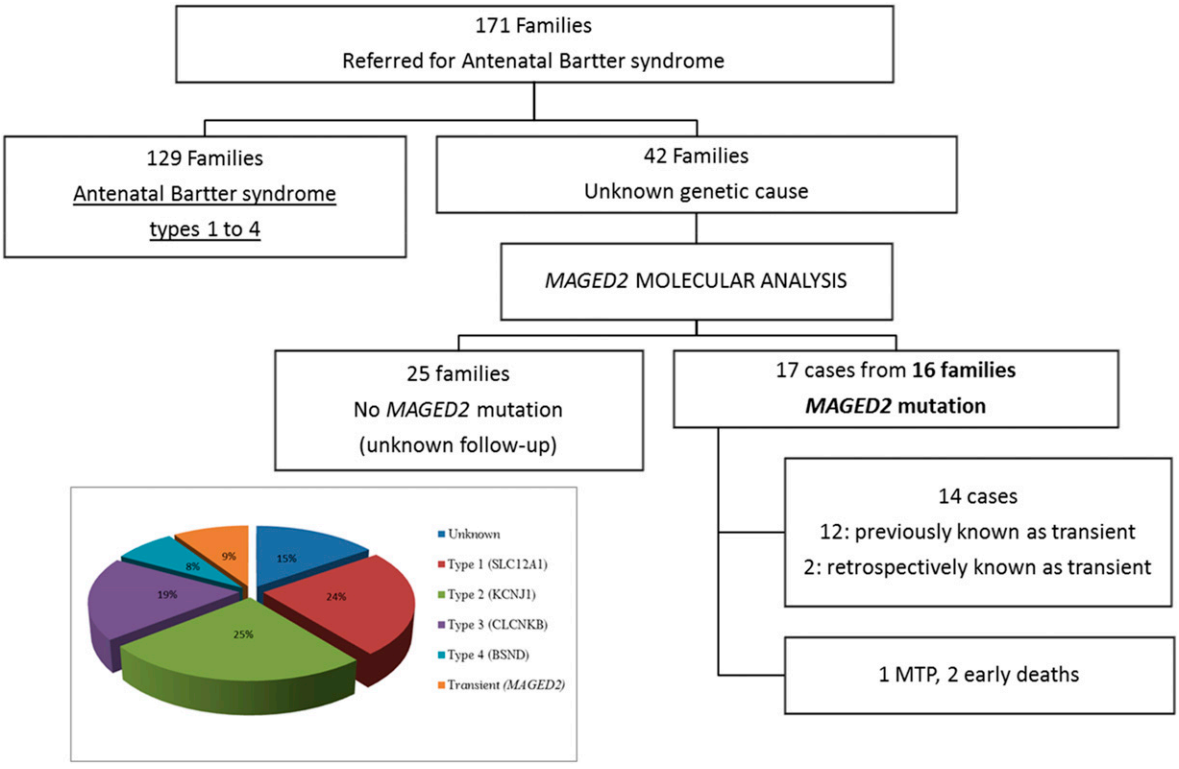

Figure 1. | ***MAGED2* mutations explained 9% of cases of antenatal Bartter syndrome**. Flowchart of the antenatal Bartter syndrome cohort and the distribution of the *MAGED2* cases according to the clinical data. In the box: genetic causes of antenatal Bartter Syndrome in French population. MTP, medical termination of pregnancy.

Table 1. *MAGED2* mutations detected in patients with transient antenatal Bartter syndrome

Family	Proband Sex	Inheritance	Nucleotide (cDNA)	Protein	Exon/Intron	Type of Mutation
F1	M	*De novo*	c.607C>T	p.Arg203Ter	e4	Nonsense
F2	M	Familial	c.842_843dup	p.Arg282GlyfsTer7	e4	Frameshift
F3	M	Familial	c.967C>T	p.Arg323Ter	e6	Nonsense
F4	M	?	c.967dup	p.Arg323ProfsTer18	e6	Frameshift
F5	M	*De novo*	c.1085+1G>A	p.?	i7	Splice (frameshift)
F6	M	?	c.1271+1G>A	p.?	i10	Splice (in frame)
F7	M	Familial	c.1336C>T	p.Arg446Cys	e11	Missense
F8	M	Familial	c.1337G>A	p.Arg446His	e11	Missense
F9	M	Familial	c.1366G>T	p.Val456Phe	e11	Missense
F10	M	Familial	c.1384_1386+4del	p.?	e11/i11	Splice (frameshift)
F11, F12	M, F	Familial	c.1420C>T	p.Gln474Ter	e12	Nonsense
F13	M	?	c.1458_1466del	p.Glu488_Ala490del	e12	In frame deletion
F14	M	?	c.1464_1475del	p.Ala490_Ala493del	e12	In frame deletion
F15	M	Familial	c.1515_1516dup	p.Gly506ValfsTer71	e12	Frameshift
F16	M	Familial	complete deletion	p.?	e1-e13	Large deletion

M, male; ?, unknown; F, female.

patterns were highly and extremely skewed in the asymptomatic daughter and mother, respectively (mutated allele mainly inactive). In F9, the X-inactivation pattern was random in the asymptomatic daughter (Supplemental Figure 3B) but could not be interpreted in the mother because the two alleles were separated by only one CAG repeat. Although the calculated ratio showed a moderately skewed X-inactivation pattern, this could be due to the contribution of one peak to the other; the stutter band from the larger allele must have overlapped the primary band of the lower allele.

Clinical Presentation

Clinical characteristics of patients with mutations are summarized in Table 3, and individual values are shown in Supplemental Figure 4. Fifteen of 17 patients were males and two were females. Severe polyhydramnios occurred in all pregnancies at 18–27 weeks of gestation, and serial amnioreductions (one to 11) were required. In four cases, polyhydramnios was present in previous or later pregnancies. Polyhydramnios was severe, with amniotic fluid index between 33 and 50 cm. Amniotic fluid biochemistry in 13 cases suggested the diagnosis of antenatal Bartter syndrome (*i.e.*, Bartter index <1) (13). In four of the current cases, indomethacin treatment was given during pregnancy for a short period.

One pregnancy resulted in medical termination. Sixteen infants were born preterm with gestational age at delivery between 26 and 33 weeks; five were extremely preterm (<28 weeks), ten were very preterm (28–32 weeks), and only the F9 case, with 11 amnioreductions, was moderately preterm (33 weeks). Birth weight percentile for gestational age was above the 90th percentile in 12 of 16 patients and above the 95th percentile in five. Birth length percentile for gestational age was above the 90th percentile in nine of 14 patients and above the 95th percentile in six. The ponderal index (PI) (PI=weight [g]×100/[height, cm]^3) (14) was below the 90th percentile for gestational age in all cases excepting F6. All infants were diagnosed in the postnatal period with Bartter syndrome with severe polyuria (median diuresis was 15 ml/kg per hour).

Surprisingly, cases F2–2 and F12–1 were females. The severity of their phenotypes and the course of the disease were comparable to those of males. Indomethacin treatment was introduced in six patients between 1 week and 4 months in the postnatal period with a mean duration of 7.5 months. Medical follow-up data were available for 13 patients. The mean follow-up was 5 years (0.4–12.5). In these cases, salt and water losses had resolved between 2 and 18 months with the end of indomethacin treatment or water and salts supplements. The means and IQR values of plasma sodium, chloride, potassium, and bicarbonate at last follow-up for 13 patients were respectively: 138 (137–139), 104 (103–105), 3.9 (3.7–4.2), and 24 (22–25) mmol/L.

Comorbidity

The associated morbidity observed in this cohort of transient antenatal Bartter syndrome is summarized in Table 4. We observed abnormalities associated with prematurity as well as other manifestations. In patients with comorbidities, high-resolution karyotype and/or comparative genomic hybridization array were normal. In the

Table 2. *MAGED2* X-inactivation patterns in females from four families

Family	Member	Phenotype	Mutated Allele (Size, bp)	WT Allele (Size, bp)	X-Inactivation Ratio	Classification of the Skewed X-Inactivation	Remark
F2	D	A	271	283	6:94	Extremely	
	M	a	271	289	65:35	Moderately	
F7	D	a	280	241	89:11	Highly	
	M	a	280	268	92:8	Extremely	
F9	D	a	283	274	57:43	Random	
	M	a	283	286	64:36	Random	Uninterpretable, alleles separated by one CAG repeat
F12	D	A	283	277	53:47	Random	
	M	a	283	283			Uninterpretable, homozygous

WT, wild type; D, daughter; A, affected; M, mother; a, asymptomatic.

patient with marfanoid appearance, mutations in the *FBN1* gene were excluded.

Two patients died in the first year of life: patient F2–1, who presented with thrombocytopenia, died at 1 month and patient F6–1, with sequels of leukomalacia, died at 12 months in a context of severe dehydration and hypernatremia. Mutations responsible for nephrogenic diabetes insipid were excluded for patient F6–1.

We compared the main characteristics of our cohort of antenatal Bartter syndrome types 1–4 with patients carrying *MAGED2* mutations (Supplemental Figure 4, Table 3). Birth weight percentile and chloremia were significantly higher in patients with *MAGED2* mutations compared with other groups. To understand this "normal or high chloremia," we therefore compared the relationship between plasma sodium and chloride concentrations between all antenatal Bartter groups. As shown in Figure 2, we confirmed the relative chloride depletion of Bartter syndrome types 3 and 4 compared with types 1 and 2; by contrast, the relationship was shifted upward in patients with *MAGED2* mutations, according to their tendency toward lower plasma bicarbonate.

We recently compared kidney function evolution in patients with different types of Bartter syndrome (15); available eGFR data at last follow-up for patients with *MAGED2* mutations was added to this comparison (Figure 3).

Discussion

Antenatal Bartter syndrome is the most severe form of Bartter syndrome; it requires close follow-up during the first 2 years of life, particularly in the neonatal period, and is associated with comorbidity linked to severe prematurity. In the presence of severe polyhydramnios, amniotic fluid biochemical tests as Bartter index can suggest this diagnosis, allowing optimization of supportive care at birth. The identification of *MAGED2* gene as responsible for an X-linked transient form of antenatal Bartter syndrome opens new perspectives for the follow-up and genetic counseling of patients and families with this syndrome.

The analysis of the *MAGED2* gene in the negative cases (n=42) of a large antenatal Bartter syndrome cohort (n=171) confirmed that the *MAGED2* gene was responsible for the transient form, which corresponded to 9% of cases in our population. We detected 15 different mutations, 13 of which had not been previously reported. Ten of these were predicted to result in the production of unstable mRNAs or truncated or absent proteins. The two previously unknown missense mutations were predicted to be pathogenic (Supplemental Table 1).

One of the main results of the analysis of our cohort was the observation of severe cases in two females, which was likely due to the extremely skewed X-inactivation pattern ratio in one case. The X-inactivation pattern was consistent with the absence of phenotype in female carriers in two families. The X-inactivation pattern could not explain the severity of the phenotype in one affected female carrier and more investigation is needed to explain her clinical manifestations. It is important to consider that the X-inactivation analysis was performed on blood samples and does not necessarily reflect the inactivation in the kidney tubules. Furthermore, methylation analysis is an indirect assessment of X-inactivation status. Lastly, the X chromosome inactivation is a complex, multiprocess phenomenon that also involves epigenetic factors such as DNA methylation, X chromosome reactivation, genes escaping inactivation, parental origin effect (imprinting), and possible elements influencing X inactivation skewness (16).

Concerning clinical presentation, our cohort demonstrated differences for some variables compared with previous cases (10). First, previously described onset of polyhydramnios was 19–20 weeks of gestation, whereas in our cohort onset occurred at 18–27 weeks. This does account for lack of difference between patients with transient antenatal Bartter syndrome and patients with types 1–4 antenatal Bartter syndrome (Supplemental Figure 4). Secondly, 12 out of the 16 patients in our cohort had weight and/or length percentiles for gestational age that were above the 90th percentile, not described previously. PI for gestational age was normal in 11 cases (harmonious macrosomia) and high in case F6

Table 3. Characteristics of patients with *MAGED2* mutations compared with antenatal Bartter syndrome types 1–4

Clinical Data (Neonatal Period)	Normal Values (When Applicable)	*MAGED2* (*n*=17)	Type 1 (SLC12A1) (*n*=41)	Type 2 (KCNJ1) (*n*=43)	Type 3 (CLCNKB)[a] (*n*=32)	Type 4a (BSND) (*n*=13)	*P* Value (Kruskal–Wallis Test)
Onset of polyhydramnios (wk of gestation)		23 (25–22)[2]	24 (22–27)[15]	25 (23–28)[16]	29 (23.5–32)[15]	22 (22–24)[8]	NS
Amniotic fluid index, cm	<24	42 (41–43)[9]	44[40]	38 and 40[41]	ND	ND	—
Bartter index		0.73 (0.52–0.86)[4]	0.64 (0.35–0.94)[33]	1.20 (0.38–1.96)[35]	1.29 (0.60–1.98)[30]	ND	—
Number of amnioreductions		2 (1–4)	2 (1–3)[5]	2 (1–4)[6]	1 (1–1)[2]	1 (1–2)[6]	—
Gestational age at delivery, wk	40	29.5 (26–31)	32 (29–34)[2]	33 (32–35)[2]	37 (36–40)	31 (28–34)[4]	*P*<0.001 B, C
Weight at birth, %	10–90	94 (86–97)	42 (14–68)[5]	49 (11–73)[6]	39 (17–70)[2]	39 (17–70)[2]	*P*<0.001 A, B, C, D
Height at birth, %	10–90	94 (85–98)[2]	72 (43–94)[20]	59 (31–984)[13]	64 (29–85)[11]	59 (35–79)[5]	*P*=0.001 B, C, D
Diuresis, ml/kg per h	1–3	15 (6–27)[1]	7 (4–13)[28]	6 (4–10)[32]	5 (3–8)[32]	5 (3–8)[26]	—
Placenta weight to birth weight ratio according to wk gestation, %		*n*=9 45 (27–75)	*n*=3 50 (30–60)	*n*=1 91	*n*=1 8	ND	—
Nephrocalcinosis at diagnosis		1[7] (10%)	19[11] (63%)	16[10] (48%)	8[8] (33%)	4[2] (36%)	*P*=0.02
Last follow-up							
Age, yr		5 (2–8)[3]	10 (7–16)[19]	13 (5–19)[7]	7 (4–12)[14]	13 (8–17)	*P*<0.01 A, B, D
Weight, %		28 (6–64)[1]	25 (4–67)[18]	7 (4–12)[26]	44 (71/10–69)[15]	44 (7–69)[15]	NS
Height, %		57 (11–82)[2]	12 (1–47)[19]	13 (3–45)[16]	16 (7–73)[15]	0.2 (0.1–73)[2]	NS
Kidney function (eGFR)		116 (104–158)[4]	71 (62–81)[11]	89 (78–99)[10]	118 (85–136)[14]	77 (32–113)[2]	*P*<0.001 A, B, D

Values are expressed as medians and interquartile ranges. Superscript values correspond to the numbers of missing data. The differences previously described between types 1–4 are represented in Supplemental Figures 1–4. ND, no data; —, not done; B, *P*<0.01 MAGED2 versus type 2; C, *P*<0.01 MAGED2 versus type 3; A, *P*<0.01 MAGED2 versus type 1; D, *P*<0.01 *MAGED2* versus type 4a.

[a]Bartter three patients with antenatal phenotype.

Table 4. Comorbidities in patients with *MAGED2* mutations

Comorbidities	*N*
Associated with prematurity	
Respiratory distress syndrome	7
Bronchopulmonary dysplasia	1
Periventricular leukomalacia	1
Intraventricular hemorrhage	2
Patent ductus arteriosus	2
Septicemia or necrotizing enterocolitis	3
Others	
Frontal bone cyst—pyloric stenosis (F3)	1
High BP. Interauricular communication and left ventricle hypertrophy (F3)	1
Marfanoid appearance, arachnodactyly, and mitral insufficiency (F7)	1
Acrodermatitis enteropathica zinc deficiency type (F4)	1
Dysmorphic facies (F2–1, F3, F9, F16)	3
Thrombocytopenia (F2–1)	1
Hydrocephalus and Chiari malformation (F9)	1
Deafness at 2 yr (F12)	1
Angioma (F5, F9)	2

N, number of patients.

(disharmonious macrosomia). Lastly, ranges of duration for salt supplements or indomethacin treatment were longer in described cases. Previously, ranges of 1–36 months and 1–9 years, respectively, were reported; in our cases, these ranges were 2–18 months and 0.75–18 months, respectively.

The comparison performed for other prenatal and biologic postnatal variables between patients with *MAGED2* mutations and other types of antenatal Bartter syndromes (Supplemental Figure 4, Table 3) showed that type 3 antenatal Bartter syndrome could be easily differentiated from transient antenatal Bartter syndrome as well as from antenatal Bartter syndrome types 1, 2, and 4. This distinction is a result of later onset of polyhydramnios, moderate prematurity, and more severe hypochloremic metabolic alkalosis as previously described (17,18). Two variables allowed differentiation between transient antenatal Bartter syndrome and all of the other types of antenatal Bartter syndromes: the birth weight percentile for gestational age and plasma chloride, which are higher in patients with *MAGED2* mutations. We have previously shown that severe hypochloremia is a hallmark of Bartter type 3; indeed, we observed a downward shift of the relationship between plasma chloride and sodium concentrations compared with types 1 and 2. This observation is consistent with a defect in adaptation to chloride depletion (15). By contrast, in most patients with *MAGED2* mutations, we observed normal or high chloremia with tendency toward lower plasma bicarbonate and the relationship between plasma chloride and sodium is shifted upward. One possible explanation is that the interaction of MAGE-D2 protein with other transport proteins in either the proximal tubule or the collecting duct results in an additional loss of sodium bicarbonate. Supporting this idea, MAGE-D2 was found by immunostaining experiments in uromodulin negative nephron segments in fetal and adult human kidney (10). In addition, the defect in bicarbonate reabsorption might explain hyperkalemia observed in few patients with *MAGED2* mutations, but unusual in other subtypes except in Bartter 2.

No other biologic variable allowed distinction between transient antenatal Bartter syndrome and antenatal Bartter

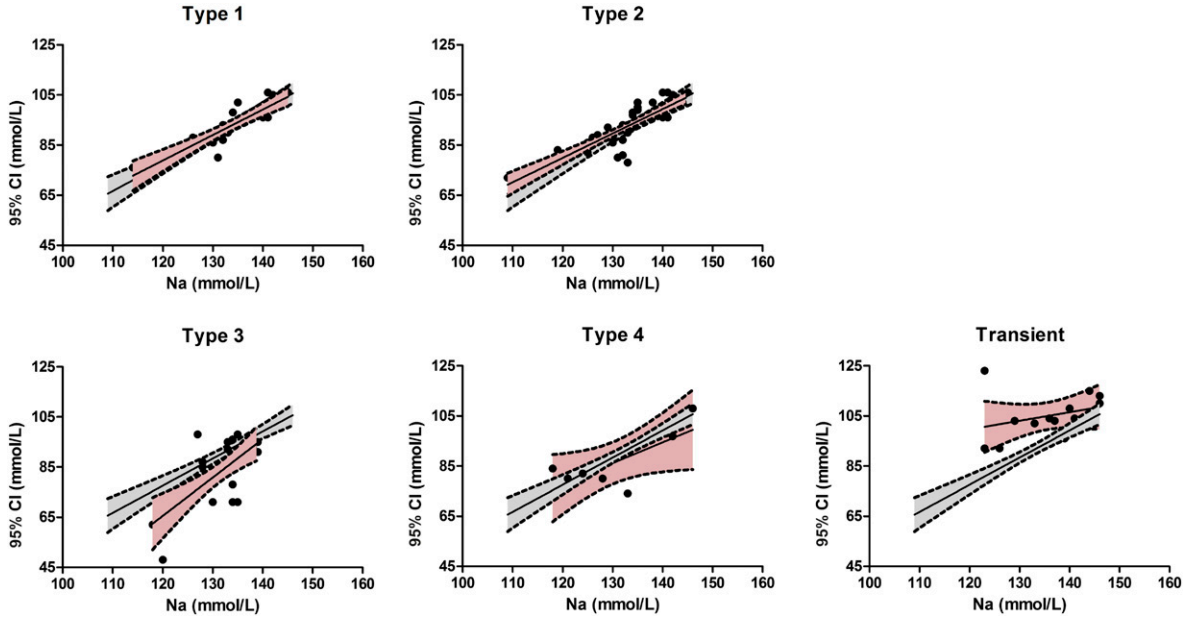

Figure 2. | Relationship between plasma sodium and plasma chloride concentrations in patients with *MAGED2* mutations is shifted upward. Data values of antenatal Bartter subtypes are presented in five separate graphs (black symbols; 95% interval of linear regression, pink area) with the linear regression of the whole population (gray area). 95% CI, 95% confidence interval.

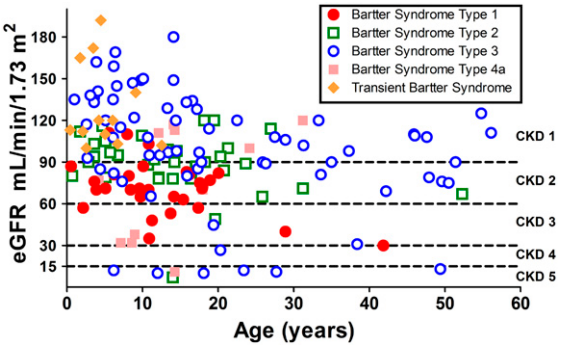

Figure 3. | Kidney function at last follow-up (or at ESRD) in patients with different types of Bartter syndrome and in patients with transient antenatal Bartter syndrome. For type 3, all phenotypes have been included (antenatal, classic, and Gitelman-like). eGFR was evaluated with Schwartz formula before 18 years and with the Modification of Diet in Renal Disease formula in adults.

syndrome type 1, which is consistent with the effect of MAGE-D2 protein on NKCC2 expression. The difficulty in differentiation highlights the important role of genetic testing during the neonatal period to guide medical decisions and to optimize follow-up. In consequence, the analysis of this gene should be included in the screening of the most severe clinical forms of antenatal Bartter syndrome, and *MAGED2* should be included in the existing next generation sequencing diagnosis panels. Furthermore, the simultaneous sequencing of all implicated genes could help to determine if *MAGED2* is a modifier gene for other Bartter syndrome types and to evaluate the existence of additional digenic inheritance.

We previously described in our Bartter syndrome cohort that CKD was observed in all Bartter syndrome types but that the proportion of patients with preserved kidney function (*i.e.*, eGFR>90 ml/min per 1.73 m^2) was higher in patients with Bartter syndrome types 2 and 3 and that moderate-to-severe kidney disease (*i.e.*, eGFR<60 ml/min per 1.73 m^2) occurred in patients with Bartter syndrome types 1 and 4 (15). Even though the age at last follow-up of patients with *MAGED2* mutations was low, all had normal eGFR.

The transient nature of this new type of Bartter syndrome remains unclear. MAGE-D2 interacts with Gs-α and HsP40; its loss of function will result in lower Gs-α activity, and inhibition of the AMPc dependent NKCC2 activity. Two mechanisms were proposed to explain the transient nature of MAGE-D2 related to Bartter syndrome: (*1*) decrease in Gs-α activity might be compensated with age by greater sensitivity to vasopressin; (*2*) tissue hypoxia in renal fetus is thought to increase endoplasmic-reticulum–associated degradation of NCC and NKCC2, which may improve after birth (10,19).

In our patients, extra kidney manifestations were observed, including harmonious macrosomia and syndromic phenotypes (Tables 3 and 4). Taking into account that MAGE proteins are ubiquitously expressed and that the MAGE-D subfamily is highly expressed in brain, it is possible that *MAGED2* mutations interfere with the expression of other proteins, explaining the syndromic presentation (20). Further explorations and fundamental studies are necessary to validate this hypothesis and to understand the transient character.

In conclusion, this work detected mutations for the *MAGED2* gene in 9% of patients in a large cohort of antenatal Bartter syndrome, a non-negligible proportion. Interestingly, clinical manifestations were observed in one female with an extremely skewed X-inactivation pattern. Transient antenatal Bartter syndrome associated with *MAGED2* mutations results in more variable clinical manifestations with a larger spectrum. However, antenatal Bartter syndromes, which now include the transient form, are often undifferentiated in the perinatal period and therefore genetic assessment should include *MAGED2* screening in routine practice.

Acknowledgments

We thank the patients and their families for agreeing to participate in this study. We thank all of the staff of the genetics laboratory of Georges Pompidou European Hospital and all of the physicians involved in the follow-up of antenatal Bartter syndrome. We thank Stephani Mazurkiewicz for her help with writing.

This work was supported by the French Ministry of Health ("Plan Maladies Rares") and the European Community (FP7EUNEFRON 201590 and European Consortium for High-Throughput Research in Rare Kidney Diseases [EURenOmics] 2012-305608).

Disclosures

None.

References

1. Bartter FC, Pronove P, Gill JR Jr., MacCardle RC: Hyperplasia of the juxtaglomerular complex with hyperaldosteronism and hypokalemic alkalosis. A new syndrome. *Am J Med* 33: 811–828, 1962
2. Rodríguez-Soriano J: Bartter and related syndromes: The puzzle is almost solved. *Pediatr Nephrol* 12: 315–327, 1998
3. Seyberth HW, Schlingmann KP: Bartter- and Gitelman-like syndromes: Salt-losing tubulopathies with loop or DCT defects. *Pediatr Nephrol* 26: 1789–1802, 2011
4. Konrad M, Vollmer M, Lemmink HH, van den Heuvel LP, Jeck N, Vargas-Poussou R, Lakings A, Ruf R, Deschênes G, Antignac C, Guay-Woodford L, Knoers NV, Seyberth HW, Feldmann D, Hildebrandt F: Mutations in the chloride channel gene CLCNKB as a cause of classic Bartter syndrome. *J Am Soc Nephrol* 11: 1449–1459, 2000
5. Simon DB, Karet FE, Hamdan JM, DiPietro A, Sanjad SA, Lifton RP: Bartter's syndrome, hypokalaemic alkalosis with hypercalciuria, is caused by mutations in the Na-K-2Cl cotransporter NKCC2. *Nat Genet* 13: 183–188, 1996
6. Simon DB, Karet FE, Rodriguez-Soriano J, Hamdan JH, DiPietro A, Trachtman H, Sanjad SA, Lifton RP: Genetic heterogeneity of Bartter's syndrome revealed by mutations in the K+ channel, ROMK. *Nat Genet* 14: 152–156, 1996
7. Simon DB, Bindra RS, Mansfield TA, Nelson-Williams C, Mendonca E, Stone R, Schurman S, Nayir A, Alpay H, Bakkaloglu A, Rodriguez-Soriano J, Morales JM, Sanjad SA, Taylor CM, Pilz D, Brem A, Trachtman H, Griswold W, Richard GA, John E, Lifton RP: Mutations in the chloride channel gene, CLCNKB, cause Bartter's syndrome type III. *Nat Genet* 17: 171–178, 1997
8. Birkenhäger R, Otto E, Schürmann MJ, Vollmer M, Ruf EM, Maier-Lutz I, Beekmann F, Fekete A, Omran H, Feldmann D, Milford DV, Jeck N, Konrad M, Landau D, Knoers NV, Antignac C, Sudbrak R, Kispert A, Hildebrandt F: Mutation of BSND causes Bartter syndrome with sensorineural deafness and kidney failure. *Nat Genet* 29: 310–314, 2001
9. Schlingmann KP, Konrad M, Jeck N, Waldegger P, Reinalter SC, Holder M, Seyberth HW, Waldegger S: Salt wasting and deafness resulting from mutations in two chloride channels. *N Engl J Med* 350: 1314–1319, 2004

10. Laghmani K, Beck BB, Yang SS, Seaayfan E, Wenzel A, Reusch B, Vitzthum H, Priem D, Demaretz S, Bergmann K, Duin LK, Göbel H, Mache C, Thiele H, Bartram MP, Dombret C, Altmüller J, Nürnberg P, Benzing T, Levtchenko E, Seyberth HW, Klaus G, Yigit G, Lin SH, Timmer A, de Koning TJ, Scherjon SA, Schlingmann KP, Bertrand MJ, Rinschen MM, de Backer O, Konrad M, Kömhoff M: Polyhydramnios, transient antenatal Bartter's syndrome, and MAGED2 mutations. *N Engl J Med* 374: 1853–1863, 2016
11. Simon DB, Nelson-Williams C, Bia MJ, Ellison D, Karet FE, Molina AM, Vaara I, Iwata F, Cushner HM, Koolen M, Gainza FJ, Gitleman HJ, Lifton RP: Gitelman's variant of Bartter's syndrome, inherited hypokalaemic alkalosis, is caused by mutations in the thiazide-sensitive Na-Cl cotransporter. *Nat Genet* 12: 24–30, 1996
12. Allen RC, Zoghbi HY, Moseley AB, Rosenblatt HM, Belmont JW: Methylation of HpaII and HhaI sites near the polymorphic CAG repeat in the human androgen-receptor gene correlates with X chromosome inactivation. *Am J Hum Genet* 51: 1229–1239, 1992
13. Garnier A, Dreux S, Vargas-Poussou R, Oury JF, Benachi A, Deschênes G, Muller F: Bartter syndrome prenatal diagnosis based on amniotic fluid biochemical analysis. *Pediatr Res* 67: 300–303, 2010
14. Roje D, Banovic I, Tadin I, Vucinović M, Capkun V, Barisic A, Vulic M, Mestrovic Z, Mimica M, Miletic T: Gestational age–the most important factor of neonatal ponderal index. *Yonsei Med J* 45: 273–280, 2004
15. Seys E, Andrini O, Keck M, Mansour-Hendili L, Courand PY, Simian C, Deschenes G, Kwon T, Bertholet-Thomas A, Bobrie G, Borde JS, Bourdat-Michel G, Decramer S, Cailliez M, Krug P, Cozette P, Delbet JD, Dubourg L, Chaveau D, Fila M, Jourde-Chiche N, Knebelmann B, Lavocat MP, Lemoine S, Djeddi D, Llanas B, Louillet F, Merieau E, Mileva M, Mota-Vieira L, Mousson C, Nobili F, Novo R, Roussey-Kesler G, Vrillon I, Walsh SB, Teulon J, Blanchard A, Vargas-Poussou R: Clinical and genetic spectrum of Bartter syndrome type 3. *J Am Soc Nephrol* 28: 2540–2552, 2017
16. Talebizadeh Z, Bittel DC, Veatch OJ, Kibiryeva N, Butler MG: Brief report: Non-random X chromosome inactivation in females with autism. *J Autism Dev Disord* 35: 675–681, 2005
17. Brochard K, Boyer O, Blanchard A, Loirat C, Niaudet P, Macher MA, Deschenes G, Bensman A, Decramer S, Cochat P, Morin D, Broux F, Caillez M, Guyot C, Novo R, Jeunemaître X, Vargas-Poussou R: Phenotype-genotype correlation in antenatal and neonatal variants of Bartter syndrome. *Nephrol Dial Transplant* 24: 1455–1464, 2009
18. Peters M, Jeck N, Reinalter S, Leonhardt A, Tönshoff B, Klaus G, Konrad M, Seyberth HW: Clinical presentation of genetically defined patients with hypokalemic salt-losing tubulopathies. *Am J Med* 112: 183–190, 2002
19. Quigley R, Saland JM: Transient antenatal Bartter's Syndrome and X-linked polyhydramnios: insights from the genetics of a rare condition. *Kidney Int* 90: 721–723, 2016
20. Lee AK, Potts PR: A comprehensive guide to the MAGE family of ubiquitin ligases. *J Mol Biol* 429: 1114–1142, 2017

Received: May 26, 2017 **Accepted:** October 2, 2017

Published online ahead of print. Publication date available at www.cjasn.org.

This article contains supplemental material online at http://cjasn.asnjournals.org/lookup/suppl/doi:10.2215/CJN.05670517/-/DCSupplemental.